Journal of Materials Chemistry C

Accepted Manuscript

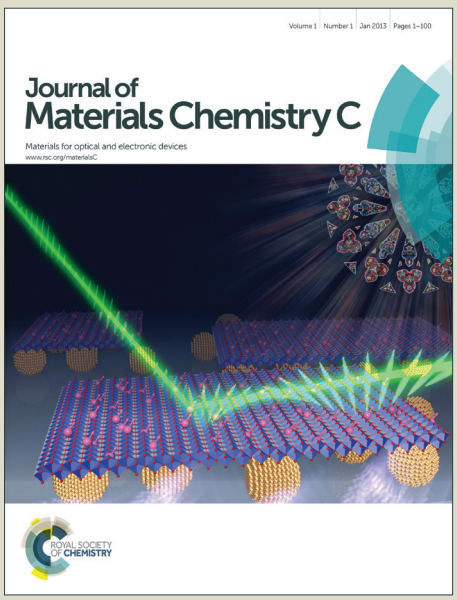

ROYAL SOCIETY OF CHEMISTRY

www.rsc.org/materialsC

Journal Name

RSCPublishing

ARTICLE

Controlling of luminescence colour through concentration of Dy^{3+} ions in $LiLa_{1-x}Dy_xP_4O_{12}$ nanocrystals

Cite this: DOI: 10.1039/x0xx00000x

Received 00th January 2012,
Accepted 00th January 2012

DOI: 10.1039/x0xx00000x

www.rsc.org/

L. Marciniak[a*], D. Hreniak[a] and W. Strek[a],

The luminescence and excitation spectra of $LiLa_{1-x}Dy_xP_4O_{12}$ nanocrystals are reported. In particular, the impact of dopant concentration on luminescence properties of $LiLa_{1-x}Dy_xP_4O_{12}$ nanocrystals was investigated. It was found that increase of Dy^{3+} concentration results in strong quenching of luminescence. The mechanism of concentration quenching was discussed in terms of the Yokota-Tanimoto model. It is concluded that, with increasing Dy^{3+} concentration, the donor-acceptor interaction leads to a significant concentration quenching resulting in nonexponential luminescence decay whereas at the high concentration limit the donor-donor interaction becomes dominant and exponential decay is observed..

Introduction

In recent few decades much effort has been put in finding and developing of new phosphors for solid state lighting applications. A great interest in this field results from a tremendous number of industrial applications where lighting plays important role. One of the most important field in solid-state lighting is related with white light generation. There are several conditions which a new phosphor should fulfill in order to consider its potential application in white light sources: high emission efficiency, color of the emitted light being close to white light (CIE coordinates close to (0.33,0.33)), good color rendering index (CRI), low temperature quenching and, finally, low cost of production. The latter condition can be fulfilled taking advantage of low cost reagents used and low cost method of synthesis of the phosphor as well. On the other hand, high chemical purity necessary for appropriate control of the physical and chemical properties of the obtained phosphor results in increase of its price. Due to relatively high quantum efficiency and well defined physical properties, which facilitate controlling of luminescence properties of the relevant phosphors, lanthanide ions have attracted great attention. One of potential candidates for generating white emission is the dysprosium ion, due to the presence of several emission bands in blue, green, yellow and red ranges of the spectrum. The emission properties of Dy^{3+} have been reported for different hosts[1-9]. The efficiency of Dy^{3+} luminescence is strongly reduced in most of crystals due to significant concentration quenching. Such quenching may be avoided in so called stoichiometric crystals[10,11] characterized by a large distance between optically active lanthanide ions.

In our previous paper, the concentration quenching effect and up-conversion emission were investigated in $LiLa_{1-x}Nd_xP_4O_{12}$[12-15]. In this paper we report the luminescence studies of lithium lanthanum tetraphosphate nanocrystals doped with dysprosium ions ($LiLa_{1-x}Dy_xP_4O_{12}$). The mean distance between two neighboring Ln^{3+} ions in fully concentrated $LiLnP_4O_{12}$ crystal is relatively large: 6 **Å**, and results in lowered concentration quenching of the luminescence. One can expect that the Dy^{3+} luminescence may be significantly enhanced in such a host even at high concentration. The mechanism of concentration quenching of luminescence is discussed.

Experimental

Nanocrystals of $LiLa_{1-x}Dy_xP_4O_{12}$ were synthesized taking advantage of a wet chemistry synthesis method described previously[12]. High purity lanthanum oxide (La_2O_3 99,99% from Stanford Materials Corporation), dysprosium oxide (Dy_2O_3 99,995% from Stanford Materials Corporation), lithium

carbonate (Li_2CO_3 99%, from POCH) and diamonium phosphate ($(NH_4)_2HPO_4$ from Sigma Aldrich) were used as a reagents. Water solutions of lanthanides nitrates, obtained by dissolving of oxides in diluted HNO_3, were mixed together with water solution of diamonium phosphate and stirred for 2h using a magnetic stirrer in order to obtain homogenous solutions. Then the solution was dried at 90°C for 24 h and this was followed by milling and calcinating at 600 °C for 6h.

The emission spectra were measured under 355 nm excitation line (3rd harmonic of YAG:Nd laser) using a Jobin-Yvon HR1000 monochromator provided with a CCD camera. The decay profiles were collected using a LeCroy WaveSurfer 400 oscilloscope.

Excitation spectra measurements were performed at room (298 K) and liquid nitrogen (77 K) temperatures using FLS920 spectrometer from Edinburgh Instruments equipped with 450 W Xenon lamp as an excitation source. It was coupled to a 275 mm excitation monochromator equipped with a 1800 l/mm grating blazed at 250 nm. The average diameter of nanocrystals was determined by the Scherrer formula from X-ray spectra. The transmission microscope images were taken using FEI Tecnai G^2 20 X-TWIN microscope supplied with with CCD FEI Eagle 2K camera. Applied voltage was 200kV. Powder diffraction studies were carried out on PANalytical X'Pert Pro diffractometer equipped using Ni-filtered Cu *Kα* radiation (V = 40 kV, I = 30 mA).

Results and discussion,

Structure and morphology

Lithium lanthanum orthophosphate ($LiLaP_4O_{12}$) crystal, which was chosen as a host material for Dy^{3+} ions, crystalizes in the monoclinic crystal system with the space group C12/c 1 (15). In order to analyze in detail the impact of concentration on spectroscopic properties of $LiLa_{1-x}Dy_xP_4O_{12}$ nanocrystals, eight samples have been synthesized with x=0.001, 0.005, 0.01, 0.1, 0.2, 0.5, 0.8, 1 of Dy^{3+} ions concentration calculated with respect to the La^{3+} ions which were replaced during doping. Powder X-ray diffraction data patterns of $LiLa_{1-x}Dy_xP_4O_{12}$ nanocrystals are presented in fig.1 a.

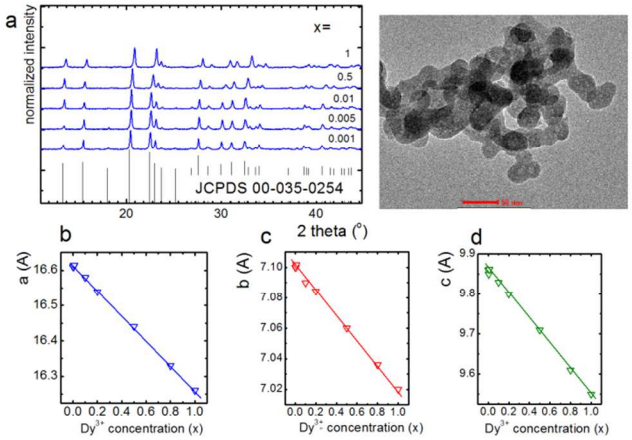

Figure 1. X-ray diffraction data of $LiLa_{1-x}Dy_xP_4O_{12}$ nanocrystals: XRD patterns a; and the impact of dopant concentration on cell parameters b, c, d. TEM image of $LiDyP_4O_{12}$ nanocrystals – e.

No evidence of additional peaks in the spectra proves the samples purity. However, one can notice a significant shifting of the diffraction peaks to higher values of 2 θ with increase of Dy^{3+} content. It is a result of reduction of the cell parameters (Fig. 1 b-d) due to the difference in ionic radiuses between host La^{3+} (130 pm for coordination number CN=8) and dopant Dy^{3+} ions (116.7 pm in CN=8) according to Vergard's rule[16]. Active ions in the host are localized in dodecahedral surrounding. Comparison of $LiLaP_4O_{12}$ and $LiDyP_4O_{12}$ matrices is shown in Table I. One can see that, in addition to cell parameters, also Ln^{3+}-O^{2-} distances are shorter in $LiDyP_4O_{12}$ host. Average size of the obtained nanocrystals was estimated from Ritveld analysis and confirmed by TEM images to be around 40 nm (Fig. 1e).

Table I. The comparison of structure parameters of $LiLaP_4O_{12}$ (ISCD 416877) and $LiDyP_4O_{12}$ (ICSD 1627851)

	$LiLaP_4O_{12}$	$LiDyP_4O_{12}$
a[Å]	16.6230	16.2600
b [Å]	7.1198	7.0259
c [Å]	9.9050	9.5783
β [°]	126.43	126.02
Ln^{3+} - O^{2-} [pm]	2.4368	2.2928
	2.4368	2.2928
	2.4823	2.3565
	2.4823	2.3565
	2.4368	2.4155
	2.4368	2.4155

Raman spectra

Room temperature Raman spectra were recorded in the range 100 – 1400 cm^{-1} (Fig 2a).

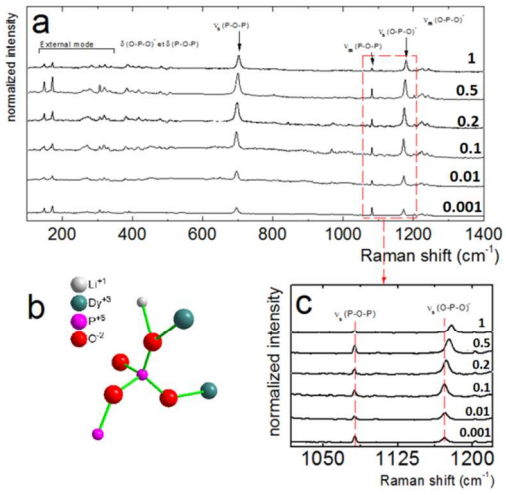

Figure 2. Raman spectra of $LiLa_{1-x}Dy_xP_4O_{12}$ nanocrystals a; visualization of P-O-P and O-P-O vibration b; and the impact of dopant concentration on energies of P-O-P and O-P-O vibrations – c.

The spectra consist of a great number of vibrations localized in the range 100-350 cm^{-1} associated with external modes. The vibration at 350-500 cm^{-1} comes from bending and breathing modes of δ(P-O-P) group followed by δO-P-O modes. One of

the most intense peaks observed is localized around 690 cm^{-1} and is a result of ν_s(P-O-P) modes. Above 1000 cm^{-1} three groups of vibrations can be found: ν_{as}(P-O-P), ν_s(O-P-O)$^-$ and ν_{as}(O-P-O)$^-$ modes.

With increase of dopant concentration shifting of ν_s(O-P-O)$^-$ mode energy can be observed while ν_{as}P-O-P is not sensitive to the Dy^{3+} amount (fig. 2c). As it can be clearly seen in Fig. 2b the ν_s(O-P-O)$^-$ mode is strongly affected by Ln^{3+} replacing. With increase of concentration of heavier Dy^{3+} ions the energy of close neighbour (O-P-O)$^-$ group increases.

It is worth to mention that one of the most intense peaks in the Raman spectra is localized for relatively large energy ~1200 cm^{-1}. Therefore, the probability of nonradiative depopulation of excited states is relatively large in tetraphosphates.

Spectroscopic characterization

Luminescence excitation spectra of $LiLa_{1-x}Dy_xP_4O_{12}$ nanocrystals were measured at 77 K and collected using λ_{mon}=575 nm as a detection line corresponding to the most intense emission line $^4F_{9/2}\rightarrow{}^4H_{13/2}$ (Fig 3a). The sharp *f-f* transition bands characteristic for Dy^{3+} ions originating from the $^6H_{15/2}$ term were observed. The most intense band was attributed to the $^6H_{15/2}\rightarrow{}^4M_{5/2}+{}^6P_{7/2}$ transition. Due to this, 355 nm excitation was used for photoluminescence measurements.

To facilitate comparison, all spectra were normalized to the intensity of the most intense $^6H_{13/2}\rightarrow{}^4M_{5/2}+{}^6P_{7/2}$ band. Although positions of bands in the excitation spectra do not change with Dy^{3+} concentration, tremendous differences in relative intensities of particular bands can be noticed. A calculation of participation of particular transitions in excitation processes was performed (Fig. 3b and c) and one can notice a decrease of $^4M_{5/2}+{}^6P_{7/2}$ and $^4P_{3/2}$ relative intensities with increase of Dy^{3+} ions number. Meanwhile, an opposite dependence can be observed in the case of lower lying (in energetic scale) transitions. This process can be explained in term of nonradiative depopulation of higher lying multiplets. The higher concentration the lower is the average Dy^{3+}-Dy^{3+} distance. Therefore, the probability of nonradiative energy transfers between ions which can take place is higher.

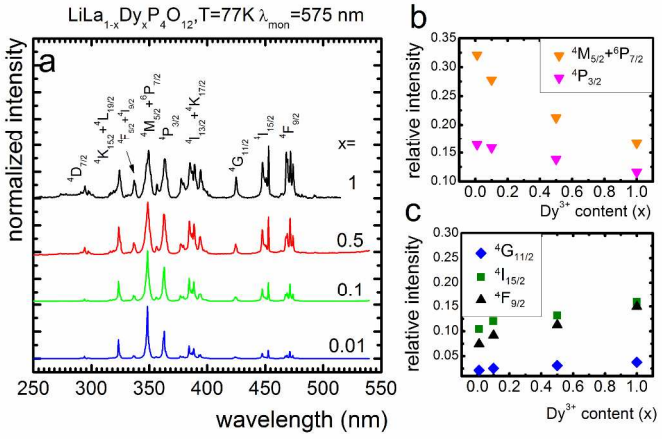

Figure 3. Excitation spectra analysis of $LiLa_{1-x}Dy_xP_4O_{12}$ nanocrystals - a; and the impact of concentration on relative intensities of excitation bands - b and - c.

The emission spectra of $LiLa_{1-x}Dy_xP_4O_{12}$ nanocrystals were measured at 300 K for different concentrations of Dy^{3+} ions (see Fig. 4a). One can notice four characteristic transition bands of Dy^{3+} originating from the $^4F_{9/2}$ state to the lower lying $^6H_{15/2}$, $^6H_{13/2}$, $^6H_{11/2}$ and $^6H_{9/2}+{}^6F_{11/2}$ terms. Two general effects of dopant concentration on emission spectra can be observed. First, the shape of the resonant $^4F_{9/2}\rightarrow{}^6H_{15/2}$ transition located around 480 nm reveals significant sensitivity to dopant concentration. Emission peaks corresponding to transition between excited $^4F_{9/2}$ and the lower Stark components of the ground $^6H_{15/2}$ decrease with increase of Dy^{3+} ions. The reason of the aforementioned behavior is reabsorption of emitted energy by neighboring Dy^{3+} ions. Probability of this process escalates with dopant concentration due to reduction of the average Dy^{3+}-Dy^{3+} distance and exhibits the highest values for those Stark components for which the population at 77 K is the highest. The second effect is tremendous extenuation of $^4F_{9/2}\rightarrow{}^6H_{9/2}+{}^6F_{11/2}$ transition intensity, localized in red range of emission spectrum. Explanation of this effect is based on reabsorption process as well and more detailed analysis of it will be presented in further discussion. The same effect was observed at room temperature as well.

Two most intense emission bands correspond to $^4F_{9/2}\rightarrow{}^6H_{15/2}$ and $^4F_{9/2}\rightarrow{}^6H_{13/2}$, however, the intensity of $^4F_{9/2}\rightarrow{}^6H_{13/2}$ located at 575 nm is dominant. Since the $^4F_{9/2}\rightarrow{}^6H_{15/2}$ transition is magnetic dipole moment allowed, its intensity does not depend on crystal field of the host. On the other hand, the intensity of $^4F_{9/2}\rightarrow{}^6H_{13/2}$, an electric dipole moment allowed band, strongly depends on local environment of the active ion and is not allowed in crystal sites of high symmetry. Therefore $^4F_{9/2}\rightarrow{}^6H_{15/2}$ to $^4F_{9/2}\rightarrow{}^6H_{13/2}$ intensity ratio can be used as a local field sensor. The fact that in the case of $LiLa_{1-x}Dy_xP_4O_{12}$ nanocrystals the intensity of $^4F_{9/2}\rightarrow{}^6H_{13/2}$ is predominant, confirms location of the active ion in low symmetry environment, without the inversion center. In order to determine the impact of the number of Dy^{3+} ions on local field symmetry, $^4F_{9/2}\rightarrow{}^6H_{15/2}$ to $^4F_{9/2}\rightarrow{}^6H_{13/2}$ parameters calculations have been performed (fig. 4 b). One can notice that, despite reduction of cell parameters with increase of dopant concentration, the dependence on local crystal field is negligible. It is also important to take into account that, in the case of higher concentration of Dy^{3+} ions, the values of this parameter are error-laden due to reduction of resonant transition intensity through reabsorption.

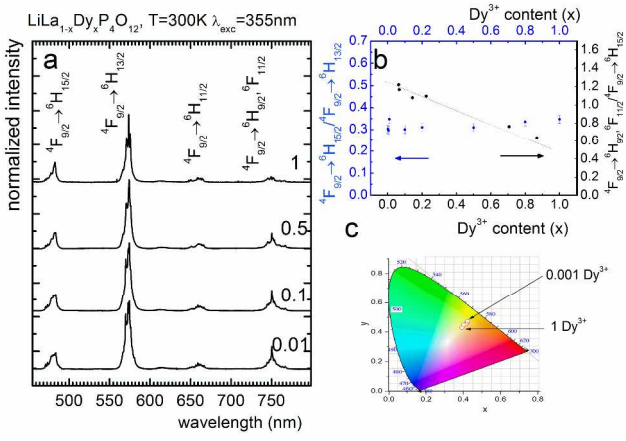

Figure 4. Luminescence spectra of $LiLa_{1-x}Dy_xP_4O_{12}$ nanocrystals - a; and the $^4F_{9/2}\rightarrow{}^6H_{15/2}$ to $^4F_{9/2}\rightarrow{}^6H_{13/2}$ intensity ratio as a function of Dy^{3+} concentration – b; and CIE coordinated obtained for $LiLa_{1-x}Dy_xP_4O_{12}$ nanocrystals.

The most intense band located at 575 nm is ascribed to the $^4F_{9/2}\rightarrow{}^6H_{13/2}$ hypersensitive transition. It does not change with concentration. An inspection of the emission features presented in the figure shows that only the intensity of $^6F_{9/2}\rightarrow{}^6H_{9/2}+{}^6F_{11/2}$ transition decreases significantly with concentration compared to other transitions. That decrease is well fitted by a linear dependence. The resonant $^4F_{9/2}\rightarrow{}^6H_{15/2}$ transition located around 480 nm reveals some insignificant increase of intensity with concentration (see Fig. 4b). The CIE coordinates obtained for these nanocrystals are presented in Fig. 4c. One can see that with increase of dopant concentration colour of emitted light shifts in the white light direction. It is a consequence of nonradiative energy transfers which takes place between Dy^{3+} ions. Therefore it is possible to altering the luminescence colour from yellowish-orange in case of diluted ions in white light direction for stoichiometric phosphors. The highest quantum yield was found for x=0.1 of Dy^{3+} ions to be 76%.

The energy diagram of electronic terms of Dy^{3+} ions with the observed fluorescence transitions and the scheme of interionic interactions between two Dy^{3+} ions are illustrated in Fig. 5. One can see that there occur two resonant interionic interactions. The first is associated with the donor-donor interaction combined with the $^4F_{9/2}\rightarrow{}^6H_{15/2}$ emission and the $^9H_{15/2}\rightarrow{}^4F_{9/2}$ absorption. The second is the donor-acceptor interaction combined with the cross relaxation via the $^6F_{9/2}\rightarrow{}^6H_{9/2}+{}^6F_{11/2}$ and $^6H_{15/2}\rightarrow{}^6F_{3/2}$ transitions.

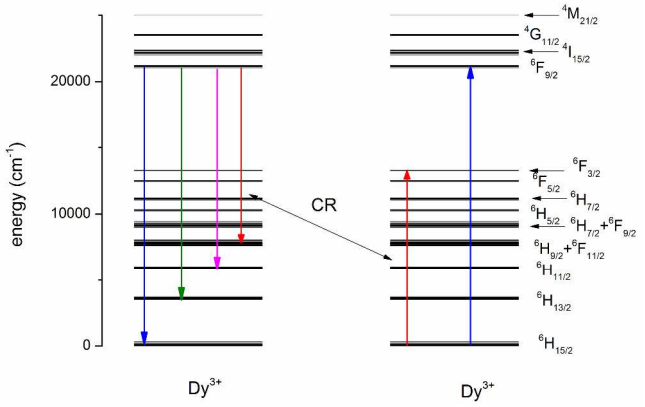

Figure 5. Energy diagram and scheme of fluorescence transitions, cross relaxation (CR) and energy migration between Dy^{3+} ions.

The kinetics of luminescence decay of the $^6F_{3/2}$ state measured at room temperature for different concentrations of Dy^{3+} ions in $LiLa_{0.9}Dy_{0.1}P_4O_{12}$ nanocrystals is shown in Fig. 6.

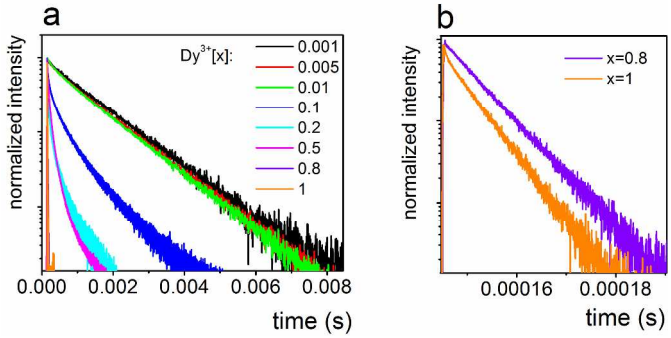

Figure 6. Luminescence decay profiles of $LiLa_{1-x}Dy_xP_4O_{12}$ nanocrystals-a and zooming on profiles of x=0.8 and x=1 of Dy^{3+} concentration - b.

One can see that for low concentration (x=0.001, 0.005, 0.01) the luminescence decays were perfectly exponential and the decay time τ_0 was determined to be 1.11 ms. Since we did not observe a significant difference with low temperature measurements, it may be treated as purely radiative lifetime. With increasing concentration (x=0. 1, 0.2, 0,3) the decay profiles became nonexponential, but for the higher concentration (x= 0.8, 1) they became again exponential (see Fig. 6b). The decay times at high concentration were determined to be 5.15 μs.

Following the energy level diagram of Dy^{3+} ion one can note that apart from the radiative and multiphonon relaxation there may occur also the cooperative donor-acceptor (DA) responsible for cross relaxation and donor-donor (DD) relaxations leading to excitation energy migration. A quantitative analysis of energy transfer phenomena in such a system is well described within the Yokota-Tanimoto theory[17] where the temporal dependence of emission intensity *I(t)* is expressed as

$$I(t)=I_0\left[\exp\left(-\frac{t}{\tau_0}\right)-\alpha\left(\frac{t}{\tau_0}\right)^{3/S}\times\left(\frac{1+10.866Z+15.50Z^2}{1+8.749Z}\right)^{(S-3)/(S-2)}\right]+b \quad (1)$$

where

$$\alpha=\frac{4}{3}\pi\Gamma\left(1-\frac{3}{s}\right)N_{Dy}R_0^3 \quad (2)$$

and

$$Z=DC_{DD}^{-2/S}t^{1-2/S} \quad (3)$$

S=6, 8, 10 for dipole-dipole, dipole-quadrupole, and quadrupole-quadrupole interactions, respectively, N_{Dy} is dopant concentration (for $LiDyP_4O_{12}$ N_{Dy}= 4.21 ·10^{21} cm^{-2}), Γ is the Euler gamma function, I_0 is initial intensity and b is the fitting offset. For dipole-dipole interaction S=6. D and C_{DD} parameters are diffusion rate and donor-donor interaction constant, respectively. The critical distance is expressed by

$$R_0=\sqrt[3]{\frac{\alpha}{\frac{4}{3}\pi\Gamma\left(1-\frac{3}{s}\right)N_A}} \quad (4)$$

and the donor-acceptor interaction parameter can be determined from the equation

$$C_{DA}=R_0^6\cdot\tau_0 \quad (5)$$

D, C_{DD} and α is the fitting parameter of decay profiles presented in fig. 4. For absence of donor-donor interaction eq. (1) can be reduced to simple Inokuti-Hirayama model[18] and hence the donor-acceptor interaction parameter can be determined for x=0.1 to be 7.10·10^{-46} [m^6/s]. For stoichiometric phosphor the decay profile becomes again exponential, due to the fast energy diffusion. Therefore, the donor-donor interaction parameter can be determined by fitting decay profile for x=1 with eq. (1) basing on the previously obtained C_{DA} parameter. Hence C_{DD} was found to be 1.03 10^{-51} [m^6/s]. The obtained value is much lower than that calculated for $LiLa_{1-x}Nd_xP_4O_{12}$ nanocrystals[12], due to the energy mismatch for cross-relaxation in this host material.

Conclusions

Synthesis and optical properties of $LiLa_{1-x}Dy_xP_4O_{12}$ nanocrystals were investigated. The impact of the amount of active ions on structure and morphology was analyzed. Reduction of cell parameters with increase of dopant concentration according to Vegards rule was observed. With increase of the dopant concentration an increase of relative

intensities corresponding to transitions from lower laying multiplets was observed and explained by multiphonon depopulation of excited states due to higher probability of nonradiative energy transfers for a higher number of Dy^{3+} ions. A significant impact of dopant concentration on luminescence emission spectra was noticed. For higher concentration of Dy^{3+} a reduction of relative intensities of emission bands corresponding to the $^4F_{9/2} \rightarrow {}^6H_{9/2}+{}^6F_{11/2}$ transition was observed. The decrease of $\beta_{6H9/2+6F11/2}$ luminescence branching ratio results from high reabsorption probability related to lowering of the average distance between Dy^{3+} ions with concentration increase. The CIE coordinates were determined. The shift of the emitted light from yellow (for low Dy^{3+} amount) in yellowish-white direction was observed. This behavior could find application for controlling the emitted light by the doping level. The impact of the dopant amount on luminescence decay profiles was analyzed in term of Yokota-Taniomoto theory.

Acknowledgements

L. M. would like to acknowledge European Social Fund of European Union for financial support. Authors would like to acknowledge prof. M. Samoc for critical reading of this paper.

Notes and references

[a] Institute for Low Temperature and Structure Research, Polish Academy of Sciences, Wroclaw, Poland.
*corresponding author: l.marciniak@int.pan.wroc.pl

1 B. Yan and X.-Q. Su, *Opt Mater,* 2007, **29,** 547.
2 G. Li, C. Li, C. Zhang, Z. Cheng, Z. Quan and C. Peng, J. Lin, *J Mater Chem*, 2007, **19,** 8936.
3 J. Pisarska, W.A. Pisarski and W. Ryba-Romanowski, *Opt Laser Technol*, 2010, **42,** 805.
4 M. Jayasimhadri, B.V. Ratnam, K. Jang, H.S. Lee, B. Chen, S.-S. Yi, J.-H. Jeong and L.R. Moorthy, *J Am Ceram Soc*, 2010, **93,** 494.
5 G. Dominiak-Dzik, W. Ryba-Romanowski, L. Kovács and E. Beregi, *Radiat Meas*, 2004, **38,** 557.
6 I. Földvári, E. Beregi, A. Baraldi, R. Capelletti, W. Ryba-Romanowski, G. Dominiak-Dzik, A. Munoz and R. Sosa, *J Lumin,* 2003, **102-103,** 395.
7 R. Martínez Vázquez, R. Osellame, M. Marangoni, R. Ramponi, E. Diéguez, M. Ferrari and M. Mattarelli, *J Phys Condens Matter*, 2004, **16,** 465.
8 W. Ryba-Romanowski, G. Dominiak-Dzik, P. Solarz and R. Lisiecki, *Opt Mat*, 2009, **31,** 1547.
9 P. Haro-González L. L. Martín I. R. Martín M. Berkowski and W. Ryba-Romanowski, *Appl Phys B,* 2011, **103,** 597.
10 W. Strek, C. Szafranski, E. Łukowiak, Z. Mazurak and B. Jeżowska-Trzebiatowska, *Phys Stat Solidi (a)*, 1977, **41,** 547.
11 H. P. Weber, *Opti Quantum Electron,* 1975, **7,** 431.
12 W. Strek, L. Marciniak, A. Lukowiak, A. Bednarkiewicz, D. Hreniak and R. Wiglusz, *Opt Mat*, 2010, **33,** 131.
13 L. Marciniak,W. Strek and D. Hreniak, *Chem Phys Lett*, 2013, **583,** 151.
14 L. Marciniak, W. Strek, A. Bednarkiewicz, A. Lukowiak and D. Hreniak, *Opt Mat*, 2011, **33,** 1492.
15 W. Strek, L. Marciniak, A. Bednarkiewicz, A. Lukowiak, D. Hreniak and R. Wiglusz, *Opt Mat,* 2010, **33,** 1097.
16 L. Vegard, *Zeitschrift für Physik,* 1921, **5,** 17.
17 T. Yokota and O. Tanimoto, *J Phys Soc Japan,* 1967, **22,** 779.
18 M. Inokuti and F. Hirayama, *J Chem Phys,* 1965, **43,** 1978.

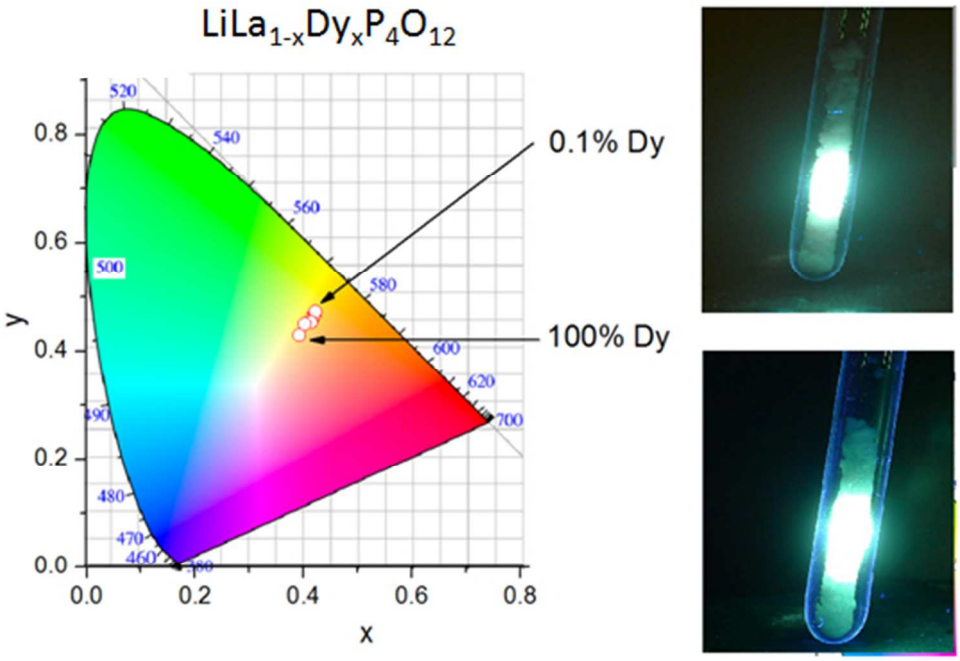

The impact of Dy concentration on CIE coordnates of LiLa1-xDyxP4O12 nanocrystals
147x100mm (96 x 96 DPI)